Molecular Dynamics Analysis of FAAH Complexed with Anandamide

Sérgio F. Sousa, João T.S. Coimbra, Pedro A. Fernandes, Tiziana Marino, Maria J. Ramos and Nino Russo

Abstract Fatty Acid Amide Hydrolase (FAAH) is a very interesting serine hydrolase that promotes the hydrolysis of both amides and esters, such as the endogenous cannabinoid anandamide or N-arachidonoyl ethanolamine (AEA), and the sleep-inducing lipid oleamide. The therapeutic potential from the pharmacological modulation of this enzyme is vast, including relevant neurological and inflammatory disorders. Different computational approaches have fallen upon the characterization of the oleamide-FAAH monomer complex. With this study, we propose a description of both the dimeric and monomeric FAAH complexes with the substrate anandamide, in order to look for relevant interactions in the active-site and differences in the monomer and dimer incorporation approaches. The study involves a comparative analysis of several important molecular aspects for which are vital not only motion but also the conformational sampling of both enzyme and substrate as well as their interaction, with the inclusion of solvent. This work comprises a flexibility analysis of FAAH through Root Mean Square Fluctuation (RMSF), Solvent Accessible Surface Accessible Area (SASA) measurements on the substrate and enzyme, Radial Distribution Functions (RDFs) of the water molecules hydrating anandamide, as well as a study on significant hydrogen bonds between the active-site residues and the substrate. The results highlight meaningful interacting residues of the FAAH active-site with the AEA substrate, and the importance of considering the dimeric complex when flexibility effects are relevant.

Keywords Fatty acid amide hydrolase · Anandamide · Molecular dynamics

S.F. Sousa · J.T.S. Coimbra · P.A. Fernandes · M.J. Ramos (✉)
REQUIMTE, Departamento de Química e Bioquímica, Faculdade de Ciências, Universidade do Porto, Rua do Campo Alegre s/n, 4169-007 Porto, Portugal
e-mail: mjramos@fc.up.pt

T. Marino (✉) · N. Russo
Dipartimento di Chimica and Centro di Calcolo ad Alte Prestazioni per Elaborazioni Parallele e Distribuite-Centro d'Eccellenza MIUR, Università della Calabria, 87030 Arcavacata di Rende, CS, Italy
e-mail: tmarino@unical.it

M.A.C. Nascimento et al. (eds.), *Frontiers in Quantum Methods and Applications in Chemistry and Physics*, Progress in Theoretical Chemistry and Physics 29,
DOI 10.1007/978-3-319-14397-2_7

1 Introduction

Fatty Acid Amide Hydrolase (FAAH) [1], first isolated from rat liver [2] is a mammalian membrane-associated enzyme that belongs to the amidase signature (AS) family, a class of serine hydrolases with a unique catalytic triad of Ser-Ser-Lys [3–7]. FAAH catalyzes the hydrolysis of both amides and esters [8]. Known substrates include anandamide (Fig. 1), an endogenous cannabinoid ligand for both cannabinoid receptors [9] and non-cannabinoid receptors [10], and oleamide, a sleep-inducing lipid originally isolated from the cerebrospinal fluid of sleep-deprived cats [11–14].

The role of FAAH in the inactivation of neuromodulatory lipid amides as well as several other experimental studies, including knockout models for the enzyme [15–28], inhibition studies [29–34], and immunohistochemical evaluations [35, 36], have confirmed FAAH as a potent potential pharmacological target to treat numerous pathophysiological conditions, such as sleep disorders, neuropathic and inflammatory pain, neurological conditions, inflammatory disorders, hypertension and even cancer [17, 37–42]. Furthermore, associations were made between polymorphisms of the *Faah* gene and disorders such as obesity [43] and drug-addiction [44]. A potential neuroprotective therapeutic profile for FAAH inhibitors has also been characterized, revealing potential against relevant neuropathological states including traumatic brain injury, Alzheimer's disease, Huntington's Disease, Parkinson's Disease, and stroke [38].

The pharmacological inhibition of FAAH has attracted great attention in recent literature, mainly due to the avoidance of unwanted side effects of the conventional cannabinoid receptors agonist's based therapy [17, 38, 45, 46]. Several classes of inhibitors for the FAAH enzyme have been described in the literature [42, 45, 47–49] and patents have been applied for, describing FAAH inhibitors [45, 46]. Several of these inhibitors are now moving, or have moved into clinical trials mainly focused on pain and inflammatory disorders. Promising results for human efficacy have been observed [45, 46, 50], with some of the inhibitors moving into clinical trials to treat anxiety and depression as a consequence [45].

FAAH is a homodimeric enzyme that exhibits a series of channels and cavities involved in the substrate binding and recognition [3, 42]. The catalytic mechanism of this enzyme involves a nucleophilic attack from the catalytic Ser241 on the carbonyl group of the substrate, forming a tetrahedral intermediate, which then

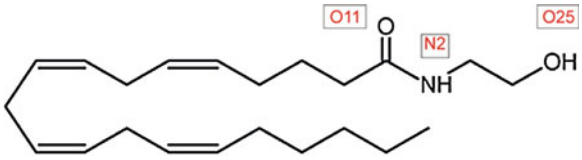

Fig. 1 The anandamide substrate: structure of the molecule with the indication of the nomenclature used to describe the oxygen and nitrogen atoms present throughout the manuscript

collapses to release the amine and the enzyme-bound acyl intermediate. Lys142 acts as a general base-general acid, mediating both the deprotonation of Ser241 and subsequent protonation of the leaving group, shuttled through Ser217. The reaction terminates with a water-mediated deacylation of the acyl enzyme-bound intermediate [4, 7, 8, 51]. The mechanistic characterization of the hydrolysis of oleamide and similar compounds has been computationally carried out with QM/MM calculations [52–56]. Furthermore, studies on drug-design computational perspectives for inhibitors of FAAH have appeared to [57–59].

The present study provides an extensive atomic-level molecular dynamics structural analysis for the FAAH-anandamide complex, of both monomer and dimerized structures of the enzyme. The intent was also to discover key players at the active site complexed with anandamide. An extensive analysis was performed on the protein stability during MD, residue flexibility, and analysis of the SASA, for both monomer and dimer complexes of FAAH-anandamide. Additionally, the water distribution around anandamide and a hydrogen bond analysis for the substrate inserted in the active site were considered.

In sum, the results provide detailed atomistic insights that include the dynamic effect of the systems and the effect of the solvent, complementing the static view that could be obtained from the X-ray structures available for this enzyme, and contributing with important indications for future mechanistic and drug-design studies on this important enzyme, allowing a better understanding of FAAH.

2 Methodology

The AMBER 10 [60] molecular dynamics package was used in all the molecular dynamics simulations performed. The monomer and dimer systems were prepared from the 1MT5 X-ray crystallographic structure of FAAH complexed with an arachidonyl inhibitor (methoxy arachidonyl fluorophosphonate) [3]. The full X-ray structure contains a total of 32 subunits, each one with 572 amino acids. A monomer and a dimer were prepared from this structure and considered for the MD study. In both systems, the substrate analogue methoxy arachidonyl fluorophosphonate was modelled into the endogenous cannabinoid substrate anandamide. The Duan et al. 2002 [61] parameters were employed to describe the protein, while the ANTECHAMBER module [62] of AMBER and the General AMBER Force Field (GAFF) [63] were used to parameterize the anandamide substrate (Fig. 1), with charges derived with RESP at the HF/6-31G(d) level of theory, to be coherent with all other parameters used.

Conventional protonation states for all amino acids at pH 7 were considered. All the hydrogen atoms were added and counter-ions (Cl^-) were employed to neutralize the positive charge of the system (ranging from −3 to −6, in the monomer and dimer studies, respectively). The Leap program was used in this regard. Each system was placed in its own rectangular box containing a minimum distance of 12 Å of TIP3P water molecules between the enzyme and the box side. The size of

these systems was of ca. 75,000 and 150,000 atoms, respectively for the monomer and dimer.

Each of the two systems was subjected to a 4-stages refinement protocol using the SANDER module of AMBER 10, in which the constraints on the enzyme were gradually removed. In the first stage (10,000 steps), 50 kcal/mol/Å^2 harmonic forces were used to restrain the positions of all atoms in the systems except those from the water molecules. In the second stage (10,000 steps) these constraints were applied only to the heavy atoms, and in the third stage (30,000 steps), they were limited to the CA and N atom-type atoms (backbone alfa carbon atoms and nitrogen atoms). This process ended with a full energy minimization (4th stage, maximum 80,000 steps) until the rms gradient was smaller than 0.02 kcal/mol/Å^2.

MD simulations were carried out using the PMEMD module of AMBER 10, and considering periodic boundary conditions to simulate a continuous system. The SHAKE algorithm [64] was applied to fix all bond lengths involving a hydrogen bond, permitting a 2 fs time step. The Particle-Mesh Ewald (PME) method [65] was used to include the long-range interactions, and a non-bond interaction cut-off radius of 10 Å was considered. Following a 40 ps equilibration procedure, 10 ns MD simulations were carried out at 310 K for each of the 2 systems (a total of 20 ns), using Langevin temperature coupling and constant pressure (1 atm) with isotropic molecule-based scaling. The MD trajectory was sampled every 2 ps. All of the MD results were analyzed with the PTRAJ module of AMBER 10.

The ConSurf server [66] was used to obtain estimated conservation grades for each amino acid position along the FAAH sequence. This server uses the initial 3-D structure of a given protein or domain (in this case the chain A in the 1MT5 PDB structure [3]) and carries out a search for close homologous sequences using the PSI-Blast [67] heuristic algorithm, with default parameters, to collect homologous sequences of a single polypeptide chain of known 3D-structure from the SWISS-PROT database [68]. These sequences are then aligned against the sequence of the initial protein with the MUSCLE algorithm [69]. A conservation score is calculated along each amino acid position using an empirical Bayesian [70] approach. The ConSurf-HSSP database may be accessed at http://consurf-hssp.tau.ac.il.

3 Results and Discussion

This section describes the broad analysis on the FAAH-anandamide complex of both monomer and dimer complexes. First, a description of the stability of both systems is shown through a Root Mean Square Displacement analysis (RMSD). Root Mean Square Fluctuation (RMSF) values on both monomer and dimer complexes are also presented, allowing an analysis on the flexibility patterns of both systems. Finally, and in order to characterize the interaction of FAAH and the anandamide substrate, SASA analysis, Radial Distribution Functions (RDFs) of the water around the substrate, and hydrogen bond analysis on the active-site are additionally conducted.

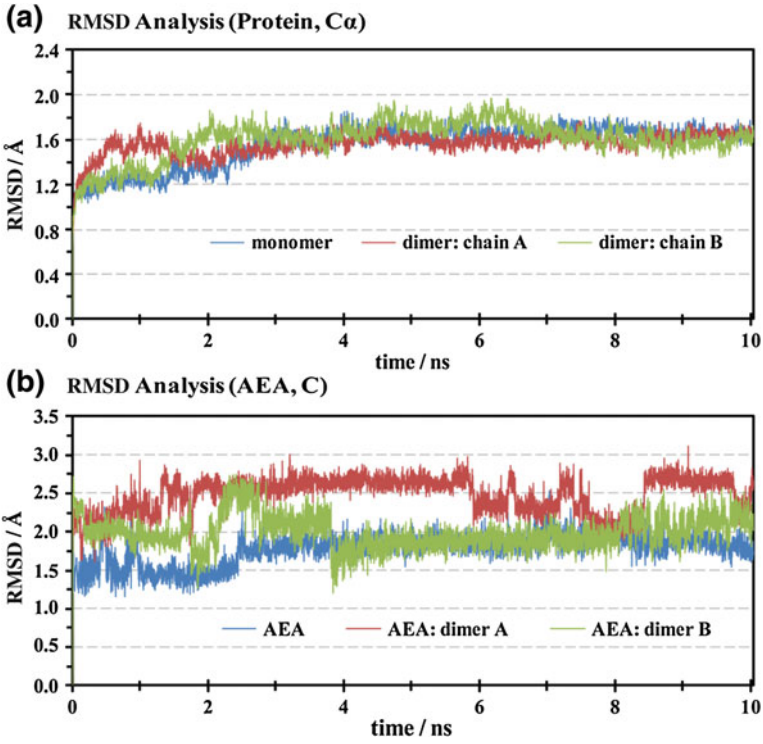

Fig. 2 **a** RMSD representation of the protein Cα atoms as a function of time for the monomer and dimer MD simulations; **b** RMSD representation of the anandamide (AEA) carbon atoms (C) as a function of time for the monomer and dimer MD simulations

3.1 Root Mean Square Deviation (RMSD) Analysis

Figure 2a shows the RMSD values for the backbone carbon atoms in the monomer and dimer MD simulations, while Fig. 2b presents the same values but for the framework of carbon atoms in the anandamide substrate in the two simulations. The results show that both the protein and the substrate molecule are well equilibrated after the initial 4 ns in both simulations. In agreement with this observation only the remaining 6 ns on both simulations were taken into consideration for the calculation of the values in the subsequent sections.

3.2 Root Mean Square Fluctuation (RMSF) Analysis

The Root mean square fluctuation values illustrate the average displacement (i.e. the positional variation) of each structural element considered in relation to their average structure over the last 6 ns of simulation, thereby giving an indication of the

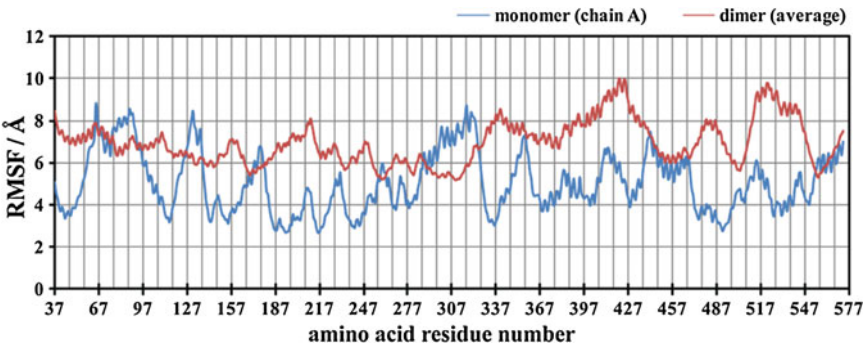

Fig. 3 RMSF analysis for all the amino acid residues along the FAAH sequence calculated for the last 6 ns of the MD simulation performed for the monomer and dimer simulation. The values for the dimer refer to the average values calculated for each residue in the two chains

relative flexibility that characterizes each of these components. In this study such analysis was performed for each amino acid residue, considering the C_α carbon atoms. Figure 3 presents the RMSF values calculated for all the amino acid residues from the MD simulation on the monomer and dimer FAAH structure.

The results highlight the existence of intrinsic differences in terms of flexibility between the several amino acid positions when treating the FAAH monomer and dimer structures. While in the monomer simulation the RMSF differences between the more flexible and the less flexible regions of the enzyme are very pronounced, in the dimer simulation there is a much higher homogeneity in terms of RMSF values along the FAAH amino acid sequence.

In the monomer structure there are 4 main flexible regions. Region 1 comprises the moderately conserved amino acids residues Gln65, Asn66 and Pro67 (with conservation scores between 6 and 8). Region 2 is defined by a stretch of 11 amino acid residue between Gln81 and Leu91. Residues in this region are in general poorly or moderately conserved, with conservation scores between 1 and 5. The only exceptions are Leu82 and Leu86 with amino acid conservation scores of 7 and 6, respectively. Region 3 is comprised by the amino acid residues Pro129, Arg130, Gln131, and Gly132. Arg130 is highly conserved (conservation score 9), while the remaining 3 residues are very poorly conserved among related sequences. Finally, region 4 is defined by a set of 9 amino acid residues, located between Arg315 and Arg323. All the residues are poorly conserved (conservation score lower than 4).

Interestingly, all these 4 regions are only moderately or poorly flexible in the RMSF analysis for the dimer. In this case, the more flexible regions are located between the amino acid residues Gly402-Ala431, and Val512-Gly544. While the more flexible regions identified in the monomer simulation refer to amino acid residues that in the functional FAAH dimer in the cell would be located opposite to the protein-membrane surface, i.e. in contact with the solvent, the more flexible regions identified in the dimer simulation refer to amino acid residues that are located in the portion of the enzyme that would interact with the cellular membrane (Fig. 4).

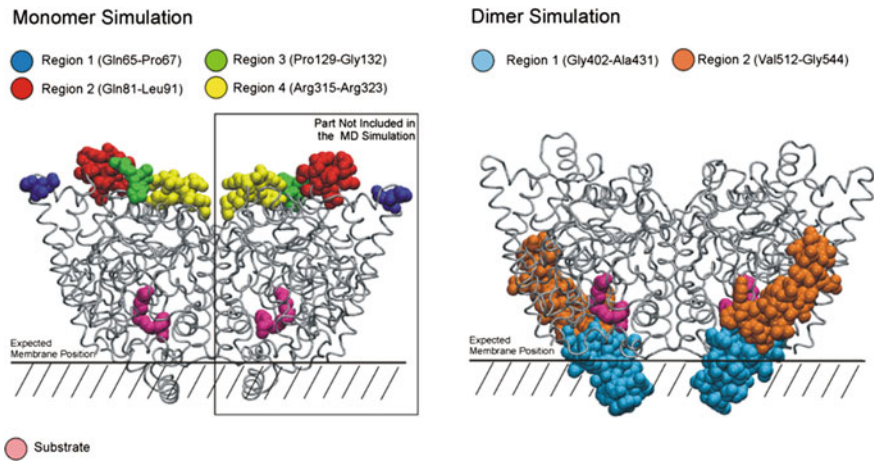

Fig. 4 Schematic representation of the most flexible regions (in terms of RMSF) identified in the monomer and dimer FAAH simulations, highlighting the differences observed for the two levels of structure considered

These observations highlight the global differences, in terms of flexibility, that exist between simulations performed on both structural elements—the FAAH monomer and the dimer. While for some more localized properties, the MD simulations performed in the monomer may be taken as a safe approximation to a more computational expensive simulation performed on the dimer, for other more global dynamic properties, such as flexibility, the inclusion of a second chain is required.

3.3 SASA Analysis

Anandamide accessible surface. SASA analysis allows an examination of the part of a given molecule that is exposed to molecules from the solvent, calculated from a probe radius that is characteristic of the solvent considered. With water, the probe radius normally considered is 1.4 Å.

The analysis performed for the anandamide substrate in the MD simulations demonstrates that this molecule is almost fully shielded from the solvent by the protein. In fact, the MD simulations performed with the monomer structure demonstrate an average SASA of only 19.2 $Å^2$ for the ligand molecule, a value that represents only 2.8 % of the total surface area of the anandamide molecule free in solution (687 ± 10 $Å^2$). Throughout the full MD simulation analyzed (3,000 configurations at 2 ps intervals), a maximum percentage of SASA of 6.2 % (44.2 $Å^2$) was observed for this molecule, while a minimum value of 0.5 % (3.5 $Å^2$) was encountered. These numbers are globally maintained in the MD simulations performed for the dimer (average SASA of 20.1 ± 6.8 $Å^2$), showing that for properties

Table 1 SASA values calculated for the anandamide molecule in the monomer and dimer simulations

	Average SASA		Maximum SASA		Minimum SASA	
Anandamide	Å^2	%	Å^2	%	Å^2	%
Monomer	19.2 ± 5.7	2.8	44.2	6.2	3.5	0.5
Dimer	20.1 ± 6.8	2.9	46.3	6.5	3.3	0.5

involving simply active-site binding of substrate (and possibly inhibitor) molecules, a single monomer is enough to guarantee a good description of the dynamics effects involved. Results are summarized in Table 1.

Anandamide contact surface. Anandamide establishes relevant van der Waals interactions with a total of 30 active-site amino acids residues, most of them of hydrophobic nature, as expected. Results are summarized in Table 2. The amino acid residues that account for most of the anandamide contact surface are Leu192 (average 11.9 %, maximum 19.3 %), Thr488 (10.6 %, 15.8 %), Phe432 (10.4 %, 15.4 %), Leu404 (9.2 %, 14.8 %), Ile491 (7.9 %, 12.4 %), and Leu380 (6.1 %, 12.6 %), as illustrated in Fig. 5. While Leu192 and Phe432 are highly conserved amino acid residues (with conservation scores of 9 and 7 respectively), the remaining residues are poorly conserved among related protein sequences.

In addition, several polar amino acid residues are in contact with the anandamide contact surface. Examples include the poorly conserved Glu373 and Ser376, and the highly conserved Arg428 and the catalytic Ser241 amino acid residues.

Protein. The calculated SASA for the monomer protein was of 22,620 ± 312 Å^2, while that of the dimer was of 40,379 ± 364 Å^2. These results demonstrate that dimer formation buries about 2,050 Å^2 per subunit, a value that represents 9 % of the surface of each subunit, resulting in an accessible surface area per monomer of 20,574 Å^2 (Table 3).

Radial Distribution Function (RDF) analysis. To have a more quantitative picture of the distribution of water molecules around the anandamide molecule we have performed a radial distribution function analysis of water (from the water oxygen atom) around the two oxygen atoms and around the nitrogen atom of the anandamide molecule, i.e. all the non-carbon and non-hydrogen atoms present in this molecule. Results are presented in Fig. 6.

The results obtained are in agreement with the SASA pattern obtained for the anandamide molecule by showing that the water molecules are in general very far away from the anandamide molecule. In fact, no water molecule is present at a distance of less than 2.45 Å from any of these three key atoms in anandamide. For the O25 and N2 atoms this water free distance can be extended to 4 Å (Fig. 6). However, the RDF analysis reveals a well defined water sphere around the O11 atom, with a maximum probability distance at 2.65 Å, corresponding to the average presence of 1 water molecule. The distance for which in average 2 water molecules are present around O11 is 5.45 Å, but at a distance of 4 Å an average number of 1.6 water molecules can be inferred (Fig. 6). Visual inspection of the MD simulation,

Table 2 Analysis of the anandamide contact surface with 30 active-site amino acid residues, with indication of the average, maximum, and minimum percentages of anandamide contact surface for each amino acid residue during the MD simulation

Interacting residue	Average percentage anandamide contact surface (%)	Maximum percentage of anandamine contact surface (%)	Minimum percentage of anandamine contact surface (%)	Amino acid conservation score
MET191	0.0 ± 0.0	0.4	0.0	8
LEU192	11.9 ± 1.9	19.3	5.2	9
SER193	0.1 ± 0.2	2.0	0.0	7
PHE194	5.2 ± 1.2	9.4	1.4	7
GLY216	0.4 ± 0.3	1.6	0.0	9
SER217	0.0 ± 0.1	0.8	0.0	9
ILE238	2.3 ± 0.9	5.9	0.1	9
GLY239	0.3 ± 0.3	2.3	0.0	9
GLY240	0.1 ± 0.2	1.0	0.0	9
SER241	0.6 ± 0.3	1.9	0.0	9
PHE244	0.9 ± 0.6	4.2	0.0	6
VAL276	2.0 ± 1.0	7.1	0.0	6
TYR335	5.2 ± 1.1	9.0	1.3	1
LEU372	4.7 ± 0.8	8.2	2.5	5
GLU373	3.3 ± 1.0	7.4	0.6	1
SER376	1.0 ± 0.5	3.6	0.0	4
ALA377	4.0 ± 1.0	8.1	0.7	5
LEU380	6.1 ± 1.8	12.6	1.4	3
PHE381	3.2 ± 1.3	8.2	0.1	5
LEU404	9.2 ± 1.6	14.8	3.5	4
ARG428	0.8 ± 0.9	6.1	0.0	7
ALA431	1.4 ± 0.6	4.4	0.0	5
PHE432	10.4 ± 1.4	15.4	6.6	7
SER435	0.1 ± 0.1	1.4	0.0	6
THR488	10.6 ± 1.5	15.8	5.3	5
GLY489	1.7 ± 0.7	4.9	0.1	3
ILE491	7.9 ± 1.3	12.4	4.4	4
SER492	0.3 ± 0.3	2.0	0.0	6
VAL495	2.8 ± 1.1	6.8	0.0	3
TRP531	3.4 ± 1.2	7.8	0.0	4

particularly in the vicinity of the O11 atom and of the MD simulation, allows the presence of 2 water molecules within a 6 Å radius of the O11 atom. These two water molecules are retained around the O11 position during the full simulation, with one of them establishing a strong hydrogen bond with the O11 atom of Anandamide during most of the simulation.

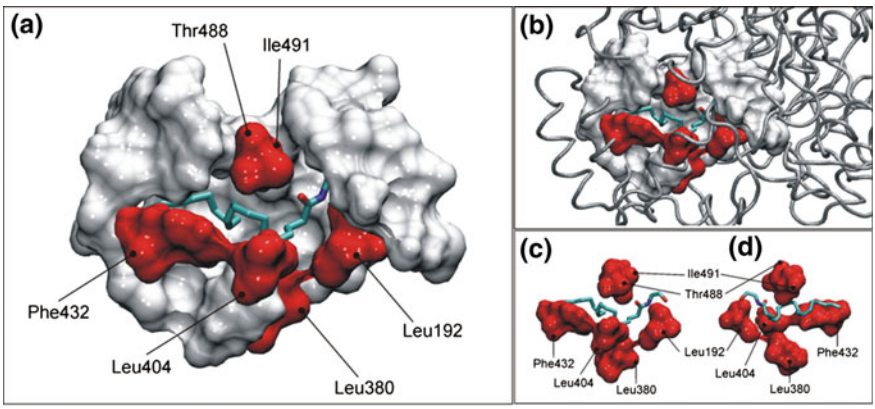

Fig. 5 Schematic representation of the anandamide contact surface prepared from the average structure in the monomer MD simulation, illustrating the binding pocket and the surface defined by the 30 interacting amino acid residues. The top 6 contact surface residues are the subject of particular attention. **a** The anandamide contact surface defined by the 30 amino acid residues; **b** Global view; **c** Top 6 residues—*front view*; **d** Top 6 residues—*rear view*

Table 3 SASA values calculated for FAAH in the monomer and dimer simulations

	Average SASA per monomer/Å^2	Maximum SASA per monomer/Å^2	Minimum SASA per monomer/Å^2
Monomer	22,620 ± 312	23,608	21,881
Dimer	20,574 ± 363	21,061	19,837

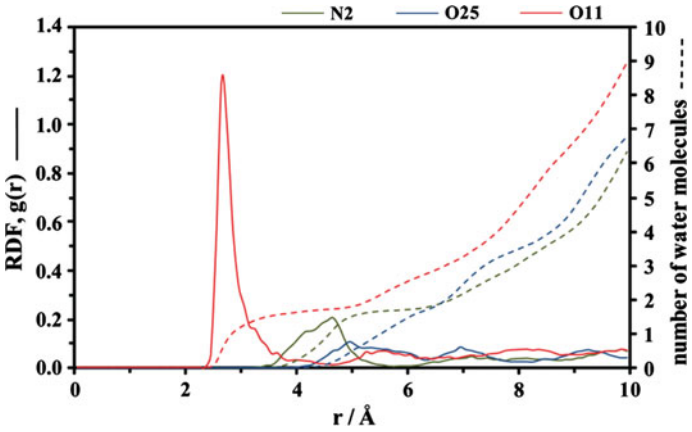

Fig. 6 Radial distribution functions (RDFs,) and number of water molecules as a function of the distance to O25, O11, and N2 atoms in anandamide calculated from the FAAH monomer simulation

Table 4 Summary of the most relevant hydrogen bonds (i.e. those present during more than 5 % of the simulation) formed between the anandamide molecule (AEA) and the active-site amino acid residues of the FAAH enzyme and water molecules (only the hydrogen bonds that were present during more than 5 % of the total simulation time are included)

Donor			Acceptor		Occupation (%)	Distance[b] (Å)	Lifetime (ps)	Max occupation (ps)
Res	Atom1	Atom2	Res	Atom1				
AEA	N2	H	Ile238	O	87.1	2.82 ± 0.09	8.7 ± 12.0	91
AEA	O25	H	Leu192	O	65.9	2.79 ± 0.11	3.8 ± 5.0	53
Wat[a]	O	H1	AEA	O11	60.2	2.70 ± 0.11	19.4 ± 30.9	190
Wat[a]	O	H2	AEA	O11	34.7	2.71 ± 0.11	10.4 ± 17.1	99
AEA	O25	H	Ser193	O	9.9	2.80 ± 0.11	1.5 ± 1.1	8

[a] The two hydrogen bonds are established with the same water molecule, but with different hydrogen atoms

[b] The distance presented refers to the distance between the two heavy atoms involved

Hydrogen Bonding (H-Bond) analysis. To obtain a more atomic-level picture of the hydrogen bonds identified in the previous section from the RDF analysis and to identify additional relevant hydrogen bonds involving the anandamide substrate we decided to perform a full-hydrogen bonding analysis.

The results (Table 4) fail to show any significant hydrogen bond between anandamide and the amino acid side chains at the active-site. Interestingly however, three hydrogen bonds with backbone oxygen atoms of highly conserved amino acid residues have been identified. These are Leu192, Ser193 and Ile238. Particular attention should be focused on the interaction with Ile238, since it is part of the oxyanion hole of the active site [55]. The backbone oxygen atom of Ile238 establishes a very important hydrogen bond, present during more than 80 % of the simulation, with the hydrogen atom connected to N2 in anandamide. Leu192 interacts through its backbone oxygen atom with the hydrogen linked to O25 in anandamide, forming a hydrogen bond that is present during ca. 65 % of the simulation. The hydrogen at O25 partially interacts also with the oxygen atom of Ser193 (Fig. 7).

As seen in the RDF analysis one water molecule establishes a strong hydrogen bond with the anandamide O11 atom. Both hydrogen atoms of this water molecule participate alternatively in this interaction, with predominance of one of these atoms (62.0 % vs. 30.5 % of occupation). No other hydrogen bonds with duration higher than 5 % of the simulation were identified between any other water molecule and anandamide.

Interestingly no relevant hydrogen bonds were found with other oxyanion hole residues (Gly239, Gly240, and Ser241) as well as with Met191, thought to be relevant in the oleamide-FAAH complex. It is also relevant the fact that the reaction catalyzed by FAAH is mediated by a high-energy state [55, 56]. Hence, this analysis could be masking relevant reactive conformations, distinct from the predominant enzyme-substrate complex here described.

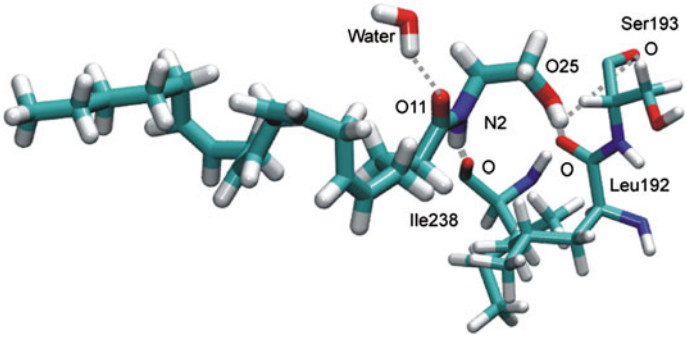

Fig. 7 Most relevant hydrogen bonds established with the anandamide substrate

4 Conclusions

Molecular modelling and molecular dynamics simulations are important tools in understanding the structure and function of biological ensembles. Molecular simulations can help to conceive and characterize conformational changes on proteins that play an essential role in their function, also providing a description at the atomic-level of the same changes. Hence, it allows the migration from a static and rigid protein structure conception to a more flexible and dynamic view. In enzymatic mechanistic studies, MD plays an important role, describing an enzyme-substrate conformational sampling, essential as a preliminary for mechanistic evaluations by methods such as QM/MM.

This study, in particular, provides a detailed analysis of key elements mediating the interaction between the FAAH enzyme and the anandamide substrate. In addition, it offers a characterization of the FAAH dimer model in contrast with the monomer, in terms of flexibility.

The results point towards pronounced differences between the flexibility profile for the monomer and dimer structures of the enzyme that could account for future considerations of the dimeric structure in future studies where the flexibility effects are relevant. Interestingly, with the monomer, the regions with higher flexibility are the regions of the enzyme with a more relevant interaction with the solvent. In the dimer case, the more flexible regions are those expected to interact with the membrane.

This study has also characterized 6 of the more relevant interacting residues in the active site with the substrate anandamide, in terms of the contact surface area. The more relevant residues ordered in terms of greater to lower extent are Leu192, Thr488, Phe432, Leu404, Ile491, and Leu380. Also, several polar amino acid residues are in contact with the anandamide surface. Examples include the poorly conserved Glu373 and Ser376, and the highly conserved Arg428 and catalytic Ser241 amino acid residues.

The analysis of RDF's and hydrogen bonding analysis accounted for 2 water molecules interacting with the anandamide substrate, as well as forming relevant hydrogen bonds through the simulation, with oxygen O11 of anandamide. Additionally, important hydrogen bonds were observed with anandamide and the residues Ile238, Ser193, Leu192 with both atoms O25 and N2 from the substrate.

The conformational and dynamics analysis of the anandamide-FAAH complex, point towards relevant active-site residue interactions with the anandamide substrate, which could be relevant in the stabilization of the substrate, and fruitful for future developments of FAAH inhibitors and enzymatic catalysis evaluations.

Acknowledgments We thank the financial support provided by FCT (PTDC/QUI-QUI/103118/2008 and grant no. Pest-C/EQB/LA0006/2011).

References

1. Schmid PC, Zuzarte-Augustin ML, Schmid HH (1985) Properties of rat liver N-acylethanolamine amidohydrolase. J Biol Chem 260(26):14145–14149
2. Cravatt BF, Giang DK, Mayfield SP, Boger DL, Lerner RA, Gilula NB (1996) Molecular characterization of an enzyme that degrades neuromodulatory fatty-acid amides. Nature 384 (6604):83–87
3. Bracey MH, Hanson MA, Masuda KR, Stevens RC, Cravatt BF (2002) Structural adaptations in a membrane enzyme that terminates endocannabinoid signaling. Science 298(5599):1793–1796
4. McKinney MK, Cravatt BF (2003) Evidence for distinct roles in catalysis for residues of the serine-serine-lysine catalytic triad of fatty acid amide hydrolase. J Biol Chem 278(39):37393–37399. doi:10.1074/jbc.M303922200
5. McKinney MK, Cravatt BF (2005) Structure and function of fatty acid amide hydrolase. Annu Rev Biochem 74:411–432. doi:10.1146/annurev.biochem.74.082803.133450
6. Giang DK, Cravatt BF (1997) Molecular characterization of human and mouse fatty acid amide hydrolases. Proc Natl Acad Sci USA 94(6):2238–2242
7. Patricelli MP, Lovato MA, Cravatt BF (1999) Chemical and mutagenic investigations of fatty acid amide hydrolase: evidence for a family of serine hydrolases with distinct catalytic properties. Biochemistry 38(31):9804–9812. doi:10.1021/bi990637z bi990637z [pii]
8. Patricelli MP, Cravatt BF (1999) Fatty acid amide hydrolase competitively degrades bioactive amides and esters through a nonconventional catalytic mechanism. Biochemistry 38 (43):14125–14130. doi:10.1021/bi991876p bi991876p [pii]
9. Devane WA, Hanus L, Breuer A, Pertwee RG, Stevenson LA, Griffin G, Gibson D, Mandelbaum A, Etinger A, Mechoulam R (1992) Isolation and structure of a brain constituent that binds to the cannabinoid receptor. Science 258(5090):1946–1949
10. Pacher P, Batkai S, Kunos G (2006) The endocannabinoid system as an emerging target of pharmacotherapy. Pharmacol Rev 58(3):389–462. doi:10.1124/pr.58.3.2 58/3/389 [pii]
11. Cravatt BF, Prospero-Garcia O, Siuzdak G, Gilula NB, Henriksen SJ, Boger DL, Lerner RA (1995) Chemical characterization of a family of brain lipids that induce sleep. Science 268 (5216):1506–1509
12. Lerner RA, Siuzdak G, Prospero-Garcia O, Henriksen SJ, Boger DL, Cravatt BF (1994) Cerebrodiene: a brain lipid isolated from sleep-deprived cats. Proc Natl Acad Sci USA 91 (20):9505–9508
13. Boger DL, Henriksen SJ, Cravatt BF (1998) Oleamide: an endogenous sleep-inducing lipid and prototypical member of a new class of biological signaling molecules. Curr Pharm Des 4 (4):303–314

14. Boger DL, Fecik RA, Patterson JE, Miyauchi H, Patricelli MP, Cravatt BF (2000) Fatty acid amide hydrolase substrate specificity. Bioorg Med Chem Lett 10(23):2613–2616
15. Lichtman AH, Shelton CC, Advani T, Cravatt BF (2004) Mice lacking fatty acid amide hydrolase exhibit a cannabinoid receptor-mediated phenotypic hypoalgesia. Pain 109(3):319–327. doi:10.1016/j.pain.2004.01.022 S0304395904000545 [pii]
16. Clement AB, Hawkins EG, Lichtman AH, Cravatt BF (2003) Increased seizure susceptibility and proconvulsant activity of anandamide in mice lacking fatty acid amide hydrolase. J Neurosci 23(9):3916–3923. doi:23/9/3916 [pii]
17. Cravatt BF, Lichtman AH (2003) Fatty acid amide hydrolase: an emerging therapeutic target in the endocannabinoid system. Curr Opin Chem Biol 7(4):469–475. doi:S1367593103000796 [pii]
18. Cravatt BF, Demarest K, Patricelli MP, Bracey MH, Giang DK, Martin BR, Lichtman AH (2001) Supersensitivity to anandamide and enhanced endogenous cannabinoid signaling in mice lacking fatty acid amide hydrolase. Proc Natl Acad Sci USA 98(16):9371–9376. doi:10.1073/pnas.161191698 161191698 [pii]
19. Wise LE, Shelton CC, Cravatt BF, Martin BR, Lichtman AH (2007) Assessment of anandamide's pharmacological effects in mice deficient of both fatty acid amide hydrolase and cannabinoid CB1 receptors. Eur J Pharmacol 557(1):44–48. doi:10.1016/j.ejphar.2006.11.002 S0014-2999(06)01262-3 [pii]
20. Osei-Hyiaman D, Depetrillo M, Harvey-White J, Bannon AW, Cravatt BF, Kuhar MJ, Mackie K, Palkovits M, Kunos G (2005) Cocaine- and amphetamine-related transcript is involved in the orexigenic effect of endogenous anandamide. Neuroendocrinology 81(4):273–282. doi:10.1159/000087925 87925 [pii]
21. Massa F, Marsicano G, Hermann H, Cannich A, Monory K, Cravatt BF, Ferri GL, Sibaev A, Storr M, Lutz B (2004) The endogenous cannabinoid system protects against colonic inflammation. J Clin Invest 113(8):1202–1209. doi:10.1172/JCI19465
22. Cravatt BF, Saghatelian A, Hawkins EG, Clement AB, Bracey MH, Lichtman AH (2004) Functional disassociation of the central and peripheral fatty acid amide signaling systems. Proc Natl Acad Sci USA 101(29):10821–10826. doi:10.1073/pnas.0401292101 0401292101 [pii]
23. Karsak M, Gaffal E, Date R, Wang-Eckhardt L, Rehnelt J, Petrosino S, Starowicz K, Steuder R, Schlicker E, Cravatt B, Mechoulam R, Buettner R, Werner S, Di Marzo V, Tuting T, Zimmer A (2007) Attenuation of allergic contact dermatitis through the endocannabinoid system. Science 316(5830):1494–1497. doi:10.1126/science.1142265 316/5830/1494 [pii]
24. Naidu PS, Varvel SA, Ahn K, Cravatt BF, Martin BR, Lichtman AH (2007) Evaluation of fatty acid amide hydrolase inhibition in murine models of emotionality. Psychopharmacology 192(1):61–70. doi:10.1007/s00213-006-0689-4
25. Moreira FA, Kaiser N, Monory K, Lutz B (2008) Reduced anxiety-like behaviour induced by genetic and pharmacological inhibition of the endocannabinoid-degrading enzyme fatty acid amide hydrolase (FAAH) is mediated by CB1 receptors. Neuropharmacology 54(1):141–150. doi:10.1016/j.neuropharm.2007.07.005 S0028-3908(07)00214-6 [pii]
26. Huitron-Resendiz S, Sanchez-Alavez M, Wills DN, Cravatt BF, Henriksen SJ (2004) Characterization of the sleep-wake patterns in mice lacking fatty acid amide hydrolase. Sleep 27(5):857–865
27. Varvel SA, Wise LE, Niyuhire F, Cravatt BF, Lichtman AH (2007) Inhibition of fatty-acid amide hydrolase accelerates acquisition and extinction rates in a spatial memory task. Neuropsychopharmacology 32(5):1032–1041. doi:10.1038/sj.npp.1301224 1301224 [pii]
28. Bambico FR, Cassano T, Dominguez-Lopez S, Katz N, Walker CD, Piomelli D, Gobbi G (2010) Genetic deletion of fatty acid amide hydrolase alters emotional behavior and serotonergic transmission in the dorsal raphe, prefrontal cortex, and hippocampus. Neuropsychopharmacology 35(10):2083–2100. doi:10.1038/npp.2010.80
29. Gobbi G, Bambico FR, Mangieri R, Bortolato M, Campolongo P, Solinas M, Cassano T, Morgese MG, Debonnel G, Duranti A, Tontini A, Tarzia G, Mor M, Trezza V, Goldberg SR, Cuomo V, Piomelli D (2005) Antidepressant-like activity and modulation of brain monoaminergic transmission by blockade of anandamide hydrolysis. Proc Natl Acad Sci USA 102(51):18620–18625. doi:10.1073/pnas.0509591102 0509591102 [pii]

30. Suplita RL, II, Farthing JN, Gutierrez T, Hohmann AG (2005) Inhibition of fatty-acid amide hydrolase enhances cannabinoid stress-induced analgesia: sites of action in the dorsolateral periaqueductal gray and rostral ventromedial medulla. Neuropharmacology 49(8):1201–1209. doi:10.1016/j.neuropharm.2005.07.007 S0028-3908(05)00263-7 [pii]
31. Lichtman AH, Leung D, Shelton CC, Saghatelian A, Hardouin C, Boger DL, Cravatt BF (2004) Reversible inhibitors of fatty acid amide hydrolase that promote analgesia: evidence for an unprecedented combination of potency and selectivity. J Pharmacol Exp Ther 311 (2):441–448. doi:10.1124/jpet.104.069401 jpet.104.069401 [pii]
32. Chang L, Luo L, Palmer JA, Sutton S, Wilson SJ, Barbier AJ, Breitenbucher JG, Chaplan SR, Webb M (2006) Inhibition of fatty acid amide hydrolase produces analgesia by multiple mechanisms. Br J Pharmacol 148(1):102–113. doi:10.1038/sj.bjp.0706699 0706699 [pii]
33. Jayamanne A, Greenwood R, Mitchell VA, Aslan S, Piomelli D, Vaughan CW (2006) Actions of the FAAH inhibitor URB597 in neuropathic and inflammatory chronic pain models. Br J Pharmacol 147(3):281–288. doi:10.1038/sj.bjp.0706510 0706510 [pii]
34. Ahn K, Johnson DS, Mileni M, Beidler D, Long JZ, McKinney MK, Weerapana E, Sadagopan N, Liimatta M, Smith SE, Lazerwith S, Stiff C, Kamtekar S, Bhattacharya K, Zhang Y, Swaney S, Van Becelaere K, Stevens RC, Cravatt BF (2009) Discovery and characterization of a highly selective FAAH inhibitor that reduces inflammatory pain. Chem Biol 16(4):411–420. doi:10.1016/j.chembiol.2009.02.013 S1074-5521(09)00080-5 [pii]
35. Egertova M, Cravatt BF, Elphick MR (2003) Comparative analysis of fatty acid amide hydrolase and cb(1) cannabinoid receptor expression in the mouse brain: evidence of a widespread role for fatty acid amide hydrolase in regulation of endocannabinoid signaling. Neuroscience 119(2):481–496. doi:S0306452203001453 [pii]
36. Long JZ, LaCava M, Jin X, Cravatt BF (2011) An anatomical and temporal portrait of physiological substrates for fatty acid amide hydrolase. J Lipid Res 52(2):337–344. doi:10.1194/jlr.M012153 jlr.M012153 [pii]
37. Schlosburg JE, Kinsey SG, Lichtman AH (2009) Targeting fatty acid amide hydrolase (FAAH) to treat pain and inflammation. AAPS J 11(1):39–44. doi:10.1208/s12248-008-9075-y
38. Hwang J, Adamson C, Butler D, Janero DR, Makriyannis A, Bahr BA (2010) Enhancement of endocannabinoid signaling by fatty acid amide hydrolase inhibition: a neuroprotective therapeutic modality. Life Sci 86(15–16):615–623. doi:10.1016/j.lfs.2009.06.003 S0024-3205(09)00262-8 [pii]
39. Fowler CJ, Jonsson KO, Tiger G (2001) Fatty acid amide hydrolase: biochemistry, pharmacology, and therapeutic possibilities for an enzyme hydrolyzing anandamide, 2-arachidonoylglycerol, palmitoylethanolamide, and oleamide. Biochem Pharmacol 62(5):517–526. doi:S0006-2952(01)00712-2 [pii]
40. Lambert DM, Fowler CJ (2005) The endocannabinoid system: drug targets, lead compounds, and potential therapeutic applications. J Med Chem 48(16):5059–5087. doi:10.1021/jm058183t
41. Ahn K, McKinney MK, Cravatt BF (2008) Enzymatic pathways that regulate endocannabinoid signaling in the nervous system. Chem Rev 108(5):1687–1707. doi:10.1021/cr0782067
42. Ahn K, Johnson DS, Cravatt BF (2009) Fatty acid amide hydrolase as a potential therapeutic target for the treatment of pain and CNS disorders. Expert Opin Drug Discov 4(7):763–784. doi:10.1517/17460440903018857
43. Sipe JC, Waalen J, Gerber A, Beutler E (2005) Overweight and obesity associated with a missense polymorphism in fatty acid amide hydrolase (FAAH). Int J Obes (Lond) 29(7):755–759. doi:10.1038/sj.ijo.0802954 0802954 [pii]
44. Sipe JC, Chiang K, Gerber AL, Beutler E, Cravatt BF (2002) A missense mutation in human fatty acid amide hydrolase associated with problem drug use. Proc Natl Acad Sci USA 99 (12):8394–8399. doi:10.1073/pnas.082235799 99/12/8394 [pii]
45. Otrubova K, Ezzili C, Boger DL (2011) The discovery and development of inhibitors of fatty acid amide hydrolase (FAAH). Bioorg Med Chem Lett 21(16):4674–4685. doi:10.1016/j.bmcl.2011.06.096 S0960-894X(11)00887-0 [pii]
46. Bachovchin DA, Cravatt BF (2012) The pharmacological landscape and therapeutic potential of serine hydrolases. Nat Rev Drug Discov 11(1):52–68. doi:10.1038/nrd3620 nrd3620 [pii]

47. Romero FA, Du W, Hwang I, Rayl TJ, Kimball FS, Leung D, Hoover HS, Apodaca RL, Breitenbucher JG, Cravatt BF, Boger DL (2007) Potent and selective alpha-ketoheterocycle-based inhibitors of the anandamide and oleamide catabolizing enzyme, fatty acid amide hydrolase. J Med Chem 50(5):1058–1068. doi:10.1021/jm0611509
48. Ahn K, Johnson DS, Fitzgerald LR, Liimatta M, Arendse A, Stevenson T, Lund ET, Nugent RA, Nomanbhoy TK, Alexander JP, Cravatt BF (2007) Novel mechanistic class of fatty acid amide hydrolase inhibitors with remarkable selectivity. Biochemistry 46(45):13019–13030. doi:10.1021/bi701378g
49. Minkkila A, Saario S, Nevalainen T (2010) Discovery and development of endocannabinoid-hydrolyzing enzyme inhibitors. Curr Top Med Chem 10(8):828–858. doi:BSP/ CTMC /E-Pub/-0051-10-8 [pii]
50. Johnson DS, Stiff C, Lazerwith SE, Kesten SR, Fay LK, Morris M, Beidler D, Liimatta MB, Smith SE, Dudley DT, Sadagopan N, Bhattachar SN, Kesten SJ, Nomanbhoy TK, Cravatt BF, Ahn K (2011) Discovery of PF-04457845: a highly potent, orally bioavailable, and selective urea FAAH inhibitor. Acs Med Chem Lett 2(2):91–96. doi:10.1021/ml100190t
51. Patricelli MP, Cravatt BF (2000) Clarifying the catalytic roles of conserved residues in the amidase signature family. J Biol Chem 275(25):19177–19184. doi:10.1074/jbc.M001607200 M001607200 [pii]
52. Tubert-Brohman I, Acevedo O, Jorgensen WL (2006) Elucidation of hydrolysis mechanisms for fatty acid amide hydrolase and its Lys142Ala variant via QM/MM simulations. J Am Chem Soc 128(51):16904–16913. doi:10.1021/ja065863s
53. Lodola A, Mor M, Hermann JC, Tarzia G, Piomelli D, Mulholland AJ (2005) QM/MM modelling of oleamide hydrolysis in fatty acid amide hydrolase (FAAH) reveals a new mechanism of nucleophile activation. Chem Commun (Camb) 35:4399–4401. doi:10.1039/b503887a
54. Capoferri L, Mor M, Sirirak J, Chudyk E, Mulholland AJ, Lodola A (2011) Application of a SCC-DFTB QM/MM approach to the investigation of the catalytic mechanism of fatty acid amide hydrolase. J Mol Model 17(9):2375–2383. doi:10.1007/s00894-011-0981-z
55. Lodola A, Sirirak J, Fey N, Rivara S, Mor M, Mulholland AJ (2010) Structural fluctuations in enzyme-catalyzed reactions: determinants of reactivity in fatty acid amide hydrolase from multivariate statistical analysis of quantum mechanics/molecular mechanics paths. J Chem Theory Comput 6(9):2948–2960. doi:10.1021/ct100264j
56. Lodola A, Mor M, Zurek J, Tarzia G, Piomelli D, Harvey JN, Mulholland AJ (2007) Conformational effects in enzyme catalysis: Reaction via a high energy conformation in fatty acid amide hydrolase. Biophys J 92(2):L20–L22. doi:10.1529/biophysj.106.098434
57. Bowman AL, Makriyannis A (2011) Approximating protein flexibility through dynamic pharmacophore models: application to fatty acid amide hydrolase (FAAH). J Chem Inf Model 51(12):3247–3253. doi:10.1021/ci200371z
58. Palermo G, Branduardi D, Masetti M, Lodola A, Mor M, Piomelli D, Cavalli A, De Vivo M (2011) Covalent inhibitors of fatty acid amide hydrolase: a rationale for the activity of piperidine and piperazine aryl ureas. J Med Chem 54(19):6612–6623. doi:10.1021/jm2004283
59. Lodola A, Mor M, Rivara S, Christov C, Tarzia G, Piomelli D, Mulholland AJ (2008) Identification of productive inhibitor binding orientation in fatty acid amide hydrolase (FAAH) by QM/MM mechanistic modelling. Chem Commun (Camb) 2:214–216. doi:10.1039/b714136j
60. Case DA, Darden TA, T. E. Cheatham I, Simmerling CL, Wang J, Duke RE, Luo R, Crowley M, Walker RC, Zhang W, Merz KM, Wang B, Hayik S, Roitberg A, Seabra G, Kolossváry I, Wong KF, Paesani F, Vanicek J, Wu X, Brozell SR, Steinbrecher T, Gohlke H, Yang L, Tan C, Mongan J, Hornak V, Cui G, Mathews DH, Seetin MG, Sagui C, Babin V, Kollman PA (2008) AMBER 10. San Francisco
61. Duan Y, Wu C, Chowdhury S, Lee MC, Xiong G, Zhang W, Yang R, Cieplak P, Luo R, Lee T, Caldwell J, Wang J, Kollman P (2003) A point-charge force field for molecular mechanics simulations of proteins based on condensed-phase quantum mechanical calculations. J Comput Chem 24(16):1999–2012. doi:10.1002/jcc.10349

62. Wang J, Wang W, Kollman PA, Case DA (2006) Automatic atom type and bond type perception in molecular mechanical calculations. J Mol Graph Model 25(2):247–260. doi:10.1016/j.jmgm.2005.12.005 S1093-3263(05)00173-7 [pii]
63. Wang J, Wolf RM, Caldwell JW, Kollman PA, Case DA (2004) Development and testing of a general amber force field. J Comput Chem 25(9):1157–1174. doi:10.1002/jcc.20035
64. Ryckaert JP, Ciccotti G, Berendsen HJ (1977) Numerical integration of the Cartesian equations of motion of a system with constraints: molecular dynamics of n-alkanes. J Comput Phys 23:327–341
65. Essmann U, Perera L, Berkowitz ML, Darden T, Lee H, Pedersen LG (1995) A smooth particle mesh Ewald method. J Chem Phys 103(19):8577–8593
66. Glaser F, Rosenberg Y, Kessel A, Pupko T, Ben-Tal N (2005) The ConSurf-HSSP database: the mapping of evolutionary conservation among homologs onto PDB structures. Proteins 58 (3):610–617. doi:10.1002/prot.20305
67. Altschul SF, Madden TL, Schaffer AA, Zhang J, Zhang Z, Miller W, Lipman DJ (1997) Gapped BLAST and PSI-BLAST: a new generation of protein database search programs. Nucleic Acids Res 25(17):3389–3402. doi:gka562 [pii]
68. Bairoch A, Apweiler R (1999) The SWISS-PROT protein sequence data bank and its supplement TrEMBL in 1999. Nucleic Acids Res 27(1):49–54. doi:gkc088 [pii]
69. Edgar RC (2004) MUSCLE: multiple sequence alignment with high accuracy and high throughput. Nucleic Acids Res 32(5):1792–1797. doi:10.1093/nar/gkh340 32/5/1792 [pii]
70. Mayrose I, Graur D, Ben-Tal N, Pupko T (2004) Comparison of site-specific rate-inference methods for protein sequences: empirical Bayesian methods are superior. Mol Biol Evol 21 (9):1781–1791. doi:10.1093/molbev/msh194 msh194 [pii]